Brushless Permanent Magnet Motor Design

Second Edition

Dr. Duane Hanselman
Electrical and Computer Engineering
University of Maine
Orono, ME 04469
USA
brushlessmotor@ieee.org
www.eece.maine.edu/motor

THE WRITERS' COLLECTIVE

Motor constant as given by (9.11) ignores the winding end turns. Since the end turns create ohmic losses but do not produce torque, they directly diminish motor constant. This fact suggests that motor constant increases at a slightly greater rate with respect to N_m than that described in the preceding paragraph. This occurs because the length of the end turns are inversely proportional to the number of magnet poles since the angular coil pitch is $2\pi/N_m$radM. The presence of end turns also suggests that motor constant decreases somewhat with increasing outside rotor radius. This occurs because end turn length is directly proportional to the distance between slots, which increases somewhat with respect to R_{ro} if R_{so} is fixed.

In summary, increasing the air gap flux density is the most significant way to increase motor constant. When the outside stator radius is fixed, the outside rotor radius plays an important but much less significant role in maximizing motor constant. Increasing the number of magnet poles plays a more significant role than the outside rotor radius but a less significant role than increasing the air gap flux density.

9.2 Cogging Torque Relationships

Cogging torque, as illustrated previously in Chapter 4, describes the desire of the permanent magnets on the rotor to align with a maximum amount of ferromagnetic material. In chapter four it was shown that integral slot motors have greater cogging torque than fractional slot motors. This occurs because the cogging torques created by the magnets add in phase alignment in integral slot motors, whereas they are out of phase with each other in fractional slot motors. In addition to identifying a number of fundamental ways to minimize cogging torque, skewing the rotor magnets or stator slots was shown to minimize cogging torque.

The fundamental properties of cogging torque described in Chapter 4 can be used to quantify the relationship among magnet pole count N_m, slot count N_s, and skew. The cogging torques experienced by all stator teeth have the same shape, but are offset from each other in phase by the angular slot pitch. Furthermore, cogging torque is periodic with respect to each magnet pole since South magnet poles create the same cogging torque as North magnet poles. As such, the fundamental frequency of the cogging torque is twice the fundamental electrical frequency whose period is one magnet pole pair. As a result, the cogging torque experienced by the *k*th stator tooth $T_{ck}(\theta)$ can be written as the Fourier series

$$T_{ck}(\theta) = \sum_{n=-\infty}^{\infty} T_n e^{jn2(\theta - k\theta_s)} \tag{9.13}$$

where T_n are the Fourier series coefficients, θ is in electrical measure, θ_s is the angular slot pitch in electrical measure, and the factor of two in the exponent reflects the fact that the fundamental cogging frequency is twice the electrical frequency.

Since the cogging torque of each tooth adds to create the net cogging torque of the motor, the motor cogging torque can be written as

$$T_{cog}(\theta) = \sum_{k=0}^{N_s-1} T_{ck}(\theta) \tag{9.14}$$

Substituting (9.13) into (9.14) and simplifying leads to

$$T_{cog}(\theta) = \sum_{n=-\infty}^{\infty} \left(T_n \Theta_n\right) e^{jn2\theta} \tag{9.15}$$

where the term in parentheses on the right hand side are the net cogging torque Fourier series coefficients and

$$\Theta_n = \sum_{k=0}^{N_s-1} e^{-j2nk\theta_s} \tag{9.16}$$

where $\theta_s = \pi N_m / N_s$ radE.

The presence of skew modifies the net cogging torque by the skew factor (7.41), which becomes

$$S_{2n} = \text{sinc}\left(\frac{n\pi N_m \alpha_{sk}}{N_s}\right) \tag{9.17}$$

when expressed in terms of twice the electrical frequency to match (9.15). Applying (9.17) to (9.15) as described in Chapter 7 gives

$$T_{cog}(\theta) = \sum_{n=-\infty}^{\infty} \left(T_n \Theta_n S_{2n}\right) e^{jn2\theta} \tag{9.18}$$

This expression describes the net cogging torque. The tooth Fourier series coefficients T_n are determined by the magnetic field distribution around each tooth, the air gap length, and the size of the slot opening between teeth. Minimizing or eliminating

cogging torque requires setting all Fourier series coefficients ($T_n\Theta_n S_{2n}$) in (9.18) to zero or minimizing the amplitude of the largest coefficients. Once the tooth Fourier series coefficients T_n are set by the chosen motor dimensions and magnet properties, minimizing or eliminating cogging torque requires study of the last two terms Θ_n and S_{2n}. For those harmonics where either of these terms are zero, the net cogging torque harmonic is zero. For example, if Θ_n is nonzero for some n, the nth cogging torque harmonic is zero if S_{2n} is zero for this n.

The zeros of S_{2n} are given by the zeros of the sinc function. Because this function is defined as $\text{sinc}(x)=\sin(x)/x$, $\text{sinc}(x)$ is zero whenever x is a nonzero multiple of π. For S_{2n} this occurs when

$$q = \frac{nN_m\alpha_{sk}}{N_s} \tag{9.19}$$

where q is any nonzero integer. When there is zero skew, *i.e.*, $\alpha_{sk}=0$, (9.19) does not hold for any q or n. This makes sense since $S_{2n}=1$ for all n when there is zero skew.

The zeros of Θ_n are not as straightforward to determine. Through careful analysis of many cases, it can be shown that in general

$$\Theta_n = \begin{cases} N_s & \text{for} \quad n = q\dfrac{\text{lcm}\left(N_s, N_m\right)}{N_m} \\ 0 & \text{otherwise} \end{cases} \tag{9.20}$$

where $\text{lcm}(x,y)$ is the least common multiple of its arguments and q is any nonzero integer that results in an integer n. Based on this result, all cogging torque harmonics are zero except those for which Θ_n is nonzero. In this case, the tooth cogging torque harmonic of all teeth simply add, making the net cogging torque a factor N_s greater than the individual tooth cogging harmonic.

For skew to be effective at eliminating cogging torque the zeros of the sinc function (9.17) must be zero at the same harmonic indices where Θ_n is nonzero. There is no need for the sinc function to be zero where Θ_n is already zero.

To investigate this possibility, consider the four pole, twelve slot motor illustrated in the cogging torque analysis conducted in Chapter 4. If a one slot pitch skew is used, *i.e.*, $\alpha_{sk}=1$, then the zeros of S_{2n} (9.17) appear at the harmonic indices

$$n=3q$$

where q is any nonzero integer. For this case, Θ_n (9.20) is nonzero at the same harmonic indices. Therefore, the zeros of the sinc function appear exactly at the correct harmonic indices to cancel cogging torque harmonics that would otherwise be nonzero. In this case, a one slot pitch skew eliminates the cogging torque.

As another example, consider the four pole, fifteen slot motor also considered in Chapter 4. If a one slot pitch skew is used, then the zeros of S_{2n} (9.17) appear at the harmonic indices

$$n = 15q$$

where q is any nonzero integer. For this case Θ_n (9.20) is nonzero at the same harmonic indices. Therefore, a one slot pitch skew eliminates the cogging torque for this case as well. In fact, a one slot pitch skew always eliminates the cogging torque. For this particular four pole, fifteen slot case, skews of one half and one quarter slot pitch also eliminate the cogging torque.

Because the indices in both (9.19) and (9.20) are harmonically related, *i.e.*, if n satisfies both relationships, then all multiples of n satisfy them also. Therefore, the minimum skew required to eliminate cogging torque can be determined by finding the first index n where both relationships hold. Doing so gives the minimum skew to eliminate cogging torque as

$$\alpha_{sk}^{*} = \frac{N_s}{\operatorname{lcm}\left(N_s, N_m\right)} \tag{9.21}$$

This minimum skew may be easier to implement mechanically and will lead to less smoothing of the tooth flux and resulting back EMF waveforms.

When skew is not used, (9.20) can be used to identify the harmonic index of the first cogging torque harmonic. If this index is n_{cog}, then the cogging torque has a fundamental frequency $2n_{cog}$ greater than the electrical frequency of the motor. The higher this harmonic frequency is, the less objectionable the cogging torque will be for two reasons. First, because the Fourier series coefficients of smooth functions generally decrease in amplitude as harmonic index increases, the higher n_{cog} is the lower the resulting cogging torque should be. And second, the higher the frequency is, the more the motor inertia filters or smoothes out the cogging torque ripple.

Study of (9.20) shows that for motors having an integral slot pitch, *i.e.*, $N_s/N_m=q$ where q is an integer, the first cogging torque harmonic index is $n_{cog}=q$. This represents the worst case situation. On the other hand, for motors having a fractional slot pitch, where N_s and N_m share no common factor, $n_{cog}=N_s$. This is the best case situa-

tion. Finally, when N_s and N_m share a common factor, *i.e.*, when the greatest common divisor gcd(N_s,N_m) is equal to some integer p, structural periodicity exists around the air gap every $360/p$°M and $n_{cog}=N_s/p$.

Given the net cogging torque Fourier series (9.18), computing the cogging torque requires computation of the cogging torque experienced by a single tooth (9.13) under zero skew conditions. Once this is known, the Fourier series coefficients T_n are easily computed. Computation of the cogging torque requires knowledge of the magnetic field entering the shoe tips in the tangential direction. That is, $B_\theta(r,\theta)$ is required in the slot openings between the stator teeth. Given this field, the tangential force density in N/m^2 on the stator teeth can be shown to be

$$f_\theta(r,\theta)=\frac{B_\theta^2(r,\theta)}{2\mu_o} \tag{9.22}$$

The torque density associated with this force density is given by the product of the force density and the radius at which it acts, *i.e.*, $T=Fr$, or

$$t_\theta(r,\theta)=\frac{B_\theta^2(r,\theta)}{2\mu_o}r \tag{9.23}$$

Integration of this torque density over the cross-sectional area of the shoe tips on both sides of a tooth gives the cogging torque. Since the force experienced on opposite sides of the tooth act in opposite directions, the cogging torque is given by the difference in force experienced by each tooth side.

The simplest way to approximate $B_\theta(r,\theta)$ is to use the circular-arc, straight-line flux flow model as shown in Fig. 9-3. With this assumption, $B_\theta(r,\theta)$ is equal to the corresponding radial magnetic field $B_{ar}(R_s,\theta)$ as given in (7.1) as modified by the slot correction factor (7.9), which is illustrated in Fig. 7-3.

Implementation of this technique for predicting cogging torque is straightforward, but the details involved are cumbersome. Because cogging torque is highly dependent on the exact form of $B_\theta(r,\theta)$, which is influenced by magnetic saturation of the shoe tip material, the accuracy of this prediction may not agree well with experimental measurements. As a result, the preceding analysis identifying harmonic content relationships of the cogging torque provides significant insight that is independent of the exact magnetic field distribution in the stator slots.

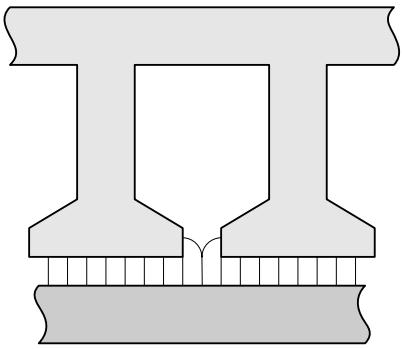

Figure 9-3. Circular-arc, straight-line flux path approximation.

In summary, the cogging torque analysis conducted here provides guidance in the selection of the number of magnet poles N_m, the number of stator slots N_s, and in the amount of skew required in a motor design. Fractional slot motors where N_m and N_s do not share a common factor exhibit the lowest cogging torque under no skew conditions. In addition, as N_m and N_s increase, the higher the fundamental cogging torque frequency becomes, making it easier for the motor inertia to filter it out.

9.3 Radial Force Relationships

In addition to undesirable tangential force, *i.e.*, cogging torque, a motor may experience an undesirable radial force between the rotor and stator that varies as the rotor rotates. As in the preceding cogging torque derivation, the force per tooth provides the basis for further analysis. In this case, the radial force experienced by the *k*th stator tooth $F_{rk}(\theta)$ can be written as the Fourier series

$$F_{rk}(\theta) = \sum_{n=-\infty}^{\infty} F_n e^{jn2(\theta - k\theta_s)} \tag{9.24}$$

where F_n are the Fourier series coefficients, θ is in electrical measure and θ_s is the angular slot pitch in electrical measure. The factor of two in the exponent reflects the fact that the fundamental radial force frequency is twice the electrical frequency because the radial force is the same over both South and North magnet poles.

The radial force on the *k*th tooth is directed at an angle $k\theta_{sm}$, where θ_{sm} is the angular slot pitch in mechanical measure. As a result, the net force experienced by the

rotor due to all teeth can be found by summing the *x*- and *y*-direction components for each tooth. Doing so leads to a net *x*-direction force of

$$F_x = \sum_{k=0}^{N_s-1} F_{rk}(\theta)\cos\left(k\theta_{sm}\right) = \sum_{n=-\infty}^{\infty} F_n X_n e^{j2n\theta} \tag{9.25}$$

where

$$X_n = \sum_{k=0}^{N_s-1} \cos\left(k\theta_{sm}\right) e^{-j2nk\theta_{se}} \tag{9.26}$$

The net *y*-direction force is

$$F_y = \sum_{k=0}^{N_s-1} F_{rk}(\theta)\sin\left(k\theta_{sm}\right) = \sum_{n=-\infty}^{\infty} F_n Y_n e^{j2n\theta} \tag{9.27}$$

where

$$Y_n = \sum_{k=0}^{N_s-1} \sin\left(k\theta_{sm}\right) e^{-j2nk\theta_{se}} \tag{9.28}$$

The effect of skew (9.17) can be included in (9.25) and (9.27). However, skew does not eliminate radial force but introduces an axial variation in the radial force and reduces its amplitude. Since this phenomenon is secondary to this discussion, skew is not considered further.

Based on (9.25) and (9.27) the rotor experiences zero radial force if both (9.26) and (9.28) are zero for all harmonic indices *n*. These two expressions are zero whenever there is geometrical symmetry between the rotor and stator around the air gap. Stated mathematically, the rotor experiences zero net radial force whenever

$$\gcd\left(N_m, N_s\right) > 1 \tag{9.29}$$

where gcd(*x*,*y*) is the greatest common divisor of its arguments. More specifically, when $\gcd(N_s,N_m)=p$ where $p>1$, symmetry exists between the rotor and stator that repeats every $360/p$°M. For example, in the four pole, twelve slot case considered earlier, gcd(12,4)=4 and the symmetry between the rotor and stator repeats every 90°M.

Since the number of magnet poles is always an even number, there is zero net radial force whenever the number of slots is also an even number. Equation (9.29) is always met in this case. On the other hand, when the number of slots is an odd integer, the rotor experiences a net radial force whenever (9.29) is not met. For example, in a four pole, fifteen slot motor, gcd(15,4)=1 and a net radial force exists. However, in a six pole, twenty-one slot motor, gcd(21,6)=3, and zero radial force exists.

In those cases where a net radial force appears, it is beneficial to know the harmonic indices that contribute to the net force since these indices identify the relative speed at which the net radial force rotates with respect to the rotor speed. The harmonic indices that contribute to the net radial force satisfy

$$n = \frac{(2q-1)N_s \pm 1}{N_m} \tag{9.30}$$

where q is a positive integer. The radial force at all other harmonic indices is zero. The harmonic indices that satisfy (9.30) do not exist for all q, nor are they uniformly spaced. For example, in a four pole, fifteen slot motor, the harmonics that satisfy (9.30) are n=4,11,19,26,..., where the difference between indices alternates between 7 and 8. For a ten pole, thirty-three slot motor, the harmonic indices that satisfy (9.30) are n=10,23,43,56,76,..., where the difference between indices alternates between 13 and 20. In both of these examples, the first contributing harmonic index is equal to N_m. However, this is not always true. For example, in an eight pole, twenty-slot motor, the harmonic indices that satisfy (9.30) are n=10,17,37,44,..., where the first contributing index is 10 rather than 8.

In addition, it is true in general that the sum of the two numbers describing the alternating differences between indices for which nonzero radial force exists always equals the number of slots N_s. For example, in the four pole, fifteen slot motor the two numbers are 7 and 8, which sum to N_s=15.

When X_n in (9.26) is nonzero, it always equals $N_s/2$. Similarly, when Y_n in (9.28) is nonzero, it equals $N_s/2$ for those indices for which (9.30) is satisfied with the minus sign. And it equals $-N_s/2$ for those indices for which (9.30) is satisfied with the plus sign. For those cases in which radial force appears, it can be computed by determining the radial force experienced by a single tooth. From the Fourier series coefficients of this force F_n, equations (9.25) through (9.28) give the desired net radial force in the x- and y-directions. The radial force on one tooth can be computed by integrating the radial force density in N/m^2

$$f_r(\theta) = \frac{B_{ar}^2(R_s, \theta)}{2\mu_o} \tag{9.31}$$

over the surface of a tooth. In (9.31), $B_{ar}(R_s,\theta)$ is given by (7.1) evaluated at the stator radius R_s at the air gap.

In summary, motors that do not have symmetry between the rotor and stator around the air gap will exhibit a net radial force having harmonic content above the fundamental electrical frequency of the motor. Since cogging torque is generally worse for motors having this symmetry, there is a tradeoff between minimum cogging torque and the presence of net radial force. In most applications, net radial force has little impact on performance. However, in low noise applications such as hard disk drive spindle motors, the presence of net radial force can limit motor acoustic performance.

9.4 Core Losses

Basic Concepts

In most motor designs, I^2R losses are the dominant contributor to reduced energy conversion efficiency. Core losses in the ferromagnetic portions of the motor are usually the next largest contributor to motor losses. As described qualitatively in Chapter 2, core loss is the sum of hysteresis and eddy current losses. These two core loss components have been studied extensively for many years. Some studies have focused on understanding and modeling the phenomena at the atomic level. Others have focused on developing core loss expressions that facilitate core loss prediction in actual devices such as motors and transformers. Still others have focused on development of new material testing procedures that facilitate accurate curve fitting of measured material properties to core loss expressions.

While the physical mechanisms that create core losses are well understood, application of this knowledge to make accurate core loss predictions remains difficult for a number of reasons. These reasons include:

- Core losses are created on a microscopic scale within a material, whereas core loss prediction uses a macroscopic scale based on assumptions of magnetic field uniformity throughout regions of the device. Therefore, the accuracy of core loss predictions depends on how well the chosen macroscopic regions model the material loss properties on a microscopic scale.

- Core loss data for many common materials is only available for 50 or 60 Hz operation using sinusoidal excitation. This 50 or 60 Hz excitation does not produce an assumed ideal sinusoidal magnetic field when using the data.
- Core loss data obtained from the commonly accepted Epstein Square Test is often of questionable value because standard test conditions do not match those of an actual motor.
- Material properties can vary by as much as 30% from batch to batch and within the same batch. In addition, they can vary within individual laminations.
- Core loss is significantly influenced by the mechanical stress and strain experienced both within the material and on its surfaces and edges. For this reason, motor laminations are often annealed after being stamped or cut. Since core loss predictions uniformly ignore this material influence, core loss predictions for nonannealed or improperly annealed laminations are invariably inaccurate.
- Since the time variation of the magnetic field distribution within a motor is seldom sinusoidal, the accuracy of core loss predictions depends on how sinusoidal excitation data is used to generate core loss expressions that apply to nonsinusoidal magnetic fields.
- Core losses are easier to predict with accuracy in regions where only the amplitude of the magnetic field changes with time, *e.g.*, in the stator tooth bodies and stator yoke sections. In regions where both the amplitude and angular direction of the magnetic field varies with time, an additional core loss component appears. That is, in addition to traditional hysteresis and eddy current loss components, the material exhibits additional *rotational losses*. This additional loss mechanism is highly dependent on the trajectory taken by the amplitude and angular motion of the magnetic field in a region. In a motor, these additional rotational losses are created in the transition area between the stator teeth and the stator yoke. Studies have shown that rotational losses can double the core losses in a region. Because of the significant work required to identify magnetic field trajectories versus time and to convert this knowledge into viable core loss expressions that vary with the trajectory shape, rotational losses are often neglected or are crudely estimated.
- Some materials exhibit an additional loss component in addition to hysteresis and eddy current components. This loss component, called the *excess* or

anomalous loss, is least understood, is difficult to determine from traditional core loss data, and is commonly ignored when predicting core losses.

Given all of these issues, core loss prediction using relatively simple modeling may indicate the correct trends from one motor design to the next but will not likely produce accurate estimates of core losses at any given operating point.

Using knowledge of the fundamental principles that cause core losses, they can be reduced by:

- Reducing the lamination thickness. Ideally, eddy current losses are directly proportional to the square of the lamination thickness. Therefore, if lamination thickness is reduced by a factor of two, eddy current losses decrease by a factor of four.
- Increasing the resistivity of the lamination material. Eddy current losses are directly proportional to material resistivity. Adding silicon to lamination steel is the most commonly adopted approach to increasing material resistivity.
- Annealing laminations after they have been stamped or cut. This eliminates the influence of mechanical stress on core loss.
- Reducing the amplitude of the magnetic field within the material. Hysteresis losses are directly proportional to the amplitude of the magnetic field raised to a power between 1.5 and 2.5. Eddy current losses are directly proportional to the square of the magnetic field amplitude. Using this property to reduce core loss is in direct conflict with maximizing torque production. As a result, other techniques for minimizing core losses are often implemented first.
- Reducing the number of magnet poles N_m. Hysteresis losses are directly proportional to the fundamental electrical frequency. Eddy current losses are directly proportional to the square of the fundamental electrical frequency. Since the fundamental electrical frequency is $N_m/2$ times greater than the motor shaft speed, reducing the magnet pole count allows one to reduce core losses significantly without lowering the motor shaft speed.

Core Loss Modeling

With the preceding information in mind, this section illustrates one approach to estimating core losses in a motor. The process develops a core loss expression that is fit to standard core loss data. Then, using expressions for the stator tooth and yoke flux densities, core losses are estimated.